

An Arctic Terrestrial Food-Chain Bioaccumulation Model for Persistent Organic Pollutants

BARRY C. KELLY AND
FRANK A. P. C. GOBAS*

School of Resource and Environmental Management,
Simon Fraser University, Burnaby,
British Columbia, Canada, V5A 1S6

A model representing the bioaccumulation of persistent organic pollutants (POPs) in arctic terrestrial mammalian food-chains is developed, parametrized, tested, and analyzed. The model predicts concentrations of POPs in lichen, caribou (*Rangifer tarandus*), and wolf (*Canis lupus*) food-chains of Canada's central and western arctic region from measured concentrations in air and snowpack meltwater. The model accounts for temporal and seasonal variation in diet composition, life-stage, body weight, and fat content over the life-span of the animal. Model predicted concentrations of 25 organic chemicals forecasted for caribou and wolves from Cambridge Bay (69°07' N 105°03' W), Inuvik (68°18' N 133°29' W) and Bathurst Inlet (64°15' N 113°07' W) are shown to be in good agreement with the observed data. The model illustrates a strong relationship between biomagnification factors and chemical K_{OA} and illustrates the effect of age, sex, and temperature on POPs bioaccumulation. Model results show that POPs with $K_{OAS} < 10^5$ do not biomagnify in arctic terrestrial food-chains, while substances that exhibit $\log K_{OAS} > 5$ and also exhibit a $\log K_{OW} > 2$, show significant bioaccumulation in arctic terrestrial food-chains. The model shows that persistent low K_{OW} ($K_{OWS} < 10^5$) but high K_{OA} substances such as β -HCH, 1,2,4,5 tetrachlorobenzene, and β -endosulfan biomagnify in terrestrial mammals.

Introduction

Aquatic food-chain bioaccumulation models have played a crucial role in the development of water and sediment quality criteria, remedial cleanup efforts, and environmental and human health risk assessments concerning persistent organic pollutants (POPs) (1, 2). Several aquatic food-chain models exist and have been adopted in regulations in the United States (3). The majority of current terrestrial food-chain bioaccumulation models are empirically derived and typically require field data to characterize food-chain bioaccumulation of organic contaminants (4, 5). Deterministic terrestrial food-chain bioaccumulation models for POPs are scarce, have not undergone field validation, and are not generally adopted. This has been cited as an important information gap in contaminant exposure and risk assessments (6). A general framework for modeling the distribution of chemical bioaccumulation in food-webs has been recently proposed by Mackay and colleagues (7), but the framework has not been applied or tested under field conditions.

It is the objective of this paper to (i) propose a model, consisting of a set of relatively simple equations, which relate aerial concentrations to resulting concentrations in arctic terrestrial food-chains and (ii) test the behavior of the model against field observations. The rationale of the study is 3-fold. First, the model provides a means to explore the behavior of this complex process by integrating a large number of recognized processes. The model allows for investigation into the significance of several simultaneously occurring processes. Second, the model embodies a hypothesis of the food-chain bioaccumulation process that can be tested. The model testing can result in suggestions for further investigation and illustrate the uncertainty associated with the model's applicability. Finally, the model provides a method for predicting the bioaccumulation behavior of chemical substances that are currently beyond the capabilities of empirical investigation. These predictions can be useful for evaluating the bioaccumulation potential of thousands of chemicals of commerce currently being assessed in Canada, the United States, and Europe under the UNEP POPs Protocol on Long-Range Transboundary Air Pollution (LRTAP), the Canadian Environmental Protection Act (CEPA), and similar legislative efforts in other countries.

The model is parametrized and applied to an arctic terrestrial food-chain involving lichens (*Cladina rangiferina* and *Cetraria nivalis*), willows (*Salix glauca*), barren-ground caribou (*Rangifer tarandus*), and wolves (*Canis lupus*). The lichen-caribou-wolf food-chain was chosen because the arctic tundra represents an environment where aerial deposition of POPs (rather than point source emission) is the predominant pathway for chemical input. Analyses of chemical dynamics in the lichen-caribou-wolf food-chain is of interest from a human health perspective as caribou are a major human food source in numerous arctic communities. Also, this arctic food-chain is comparable to the pasture-cow-human food-chain in temperate regions.

Theory

General. The model consists of a series of mechanistic equations relating ambient concentrations of organic contaminants to resulting concentrations in arctic vegetation, herbivores, and carnivorous predators (Figure 1). Input parameters are compiled, and the model is used to estimate concentrations of a series of POPs in vegetation (lichens and willows), caribou, and wolves from observed aerial and snowpack concentrations. The model is then tested by comparison of model-predicted and observed concentrations.

Air-to-Vegetation Distribution Model. Models of varying complexity have been developed to describe the bioaccumulation of organic chemicals in vegetation (8–11). An extensive review of POPs uptake in plants by McLachlan (12) suggests a homogeneous one-compartment model has proven adequate for modeling the uptake and elimination of POPs in vegetation. Three dominant processes have so far been recognized to affect the exchange of POPs between the atmosphere and arctic vegetation. The first process is the air-to-vegetation partitioning of chemical in the gaseous form in the atmosphere (5, 13, 14). The second process is the direct deposition and erosion of chemical associated with particulate matter in the atmosphere. This can include both dry particulate fallout and wet deposition (e.g., scavenging via rain or snow). This is a nondiffusive bioaccumulation mechanism, particularly important for chemicals that exhibit high octanol-air partition coefficients (K_{OA}) such as PAHs, dioxins, and highly chlorinated biphenyls because these

* Corresponding author phone: (604)291-5928; fax: (604)291-4968; e-mail: gobas@sfu.ca.

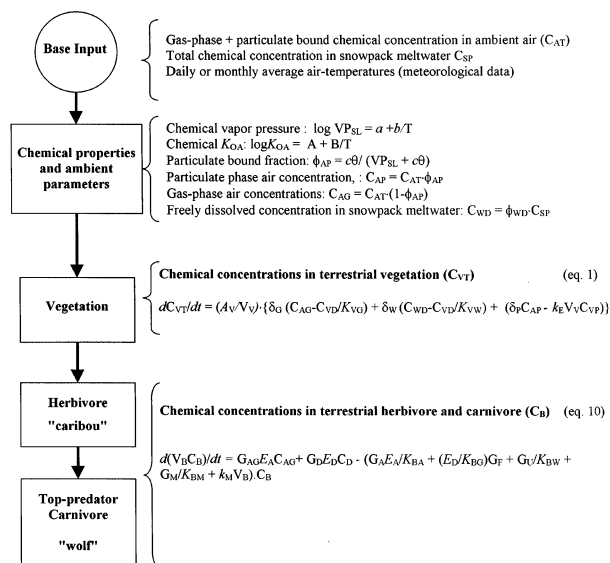


FIGURE 1. Schematic illustration of the modeling framework, including base input parameters, chemical properties and ambient parameters and the various model equations.

substances occur predominantly in a particulate-bound state in the gas phase (15, 16). The third process is the precipitation and subsequent accumulation of chemical from overlying snowpacks via water-to-vegetation partitioning during snowmelt events (17). Lichens may be particularly susceptible to this route of exposure because unlike vascular plants that are dormant during winter months, the leaf surface area of lichens is directly exposed to spring meltwater during snowmelt events. The following equation can be used to describe this model

$$dC_{VT}/dt = (A_V/V_V) \cdot \{ \delta_G (C_{AG} - C_{VD}/K_{VG}) + \delta_W (C_{WD} - C_{VD}/K_{VW}) + (\delta_P C_{AP} - k_E V_V C_{VP}) \} \quad (1)$$

where V_V is the volume of vegetation (m^3), C_{VT} is the total concentration in the vegetation ($mol \cdot m^{-3}$), and A_V is the projected leaf surface area (m^2). C_{VD} is the absorbed concentration in vegetation ($mol \cdot m^{-3}$). δ_G and δ_W ($m \cdot h^{-1}$) are mass transfer coefficients for air-to-vegetation diffusion and meltwater to vegetation diffusion, respectively. δ_P is the deposition velocity ($m \cdot h^{-1}$) of particle bound chemical to the leaf surface and lumps together both wet and dry deposition. C_{AG} ($mol \cdot m^{-3}$) is the gas-phase concentration of airborne chemical, and C_{WD} ($mol \cdot m^{-3}$) is the freely dissolved concentration in meltwater. K_{VG} and K_{VW} are the vegetation-gas-phase partition coefficient and vegetation-water partition coefficient at the ambient temperature, respectively. C_{VP} is the adsorbed vegetation concentration due to particulate deposition ($mol \cdot m^{-3}$) adhering to the vegetation surface, C_{AP} is the particulate-bound concentration of ambient air ($mol \cdot m^{-3}$), and k_E is the first-order rate constant for erosion of particle-bound chemical once associated with the vegetation surface.

To estimate the atmosphere-vegetation exchange of airborne contaminants it is necessary to quantify particle-gas partitioning and hence the phase distribution of chemical in ambient air. Gas-phase concentrations are required to assess air-to-vegetation partitioning, while particulate-bound concentrations aid the assessment of deposition rates and precipitation scavenging efficiencies (18). The latter has proven particularly important for snowfall scavenging and subsequent snowpack accumulation of airborne organic contaminants in northern and alpine ecosystems (19, 20). The fraction of total airborne chemical sorbed to aerosols

(ϕ_{AP}) can be estimated using the Junge-Pankow model (16, 21)

$$\phi_{AP} = c\theta / (VP_{SL} + c\theta) \quad (2)$$

where θ is the aerosol surface area ($cm^2 \cdot cm^{-3}$ air) and c is the chemical adsorption parameter to aerosols (Pa-cm) and is approximately 17.2 Pa-cm for POPs (16) and VP_{SL} is the chemical's vapor pressure (Pa) of the supercooled liquid, which is related to temperature by the Clausius-Clapeyron equation

$$\log VP_{SL} = a + b/T \quad (3)$$

where T is absolute temperature (Kelvin), and a and b are experimentally derived and exist for a number of POPs (21, 22). The atmospheric chemical concentration in the particulate phase (C_{AP}) and gas phase (C_{AG}) can then be calculated for a given ambient condition as $C_{AP} = C_{AT} \cdot \phi_{AP}$ and $C_{AG} = C_{AT} \cdot (1 - \phi_{AP})$ where C_{AT} ($mol \cdot m^{-3}$) is the total concentration measured in air (gas + particle).

The air-vegetation and water-vegetation partition coefficients K_{VG} and K_{VW} are dependent on the sorptive capacities of air, water, and vegetation. Recent evidence indicates that the sorptive capacity of vegetation ranges widely between species and cannot be readily estimated from the plant's lipid content (23). We propose that a three-phase partitioning model, which recognizes the sorptive capacities of the lipids (subscript L), nonlipid organic matter (subscript N), and water (subscript W) in vegetation, can be used to estimate the partitioning of POPs in certain types of arctic vegetation including lichens and willow leaves using the equations

$$K_{VG} = (\nu_L + 0.035 \cdot \nu_N) K_{OA} + \nu_W / K_{AW} \quad \text{and} \\ K_{VW} = (\nu_L + 0.035 \cdot \nu_L) K_{OW} + \nu_W \quad (4)$$

where ν_L is the lipid content, ν_N is the nonlipid organic matter content, and ν_W is the water content of the vegetation. The constant 0.035 represents the smaller sorptive capacity of the organic fraction of the vegetation (excluding the lipids) compared to that of the lipid fraction of the vegetation. The value is based on findings of the sorptive capacity of nonlipid organic matter in fish diets (24) and should be viewed as an initial estimate for the sorptive capacity of nonlipid organic matter in arctic vegetation in absence of better data. Chemical K_{OA} , K_{OW} , and K_{AW} are temperature dependent (25-28). Recent investigations have shown the effect of temperature on chemical K_{OA} can be substantial (25, 26). $\log K_{OA}$ is expressed as a function of temperature by the equation

$$\log K_{OA} = A_{OA} + B_{OA}/T \quad (5)$$

where T is absolute temperature (Kelvin) and A_{OA} and B_{OA} are compound specific parameters, documented for certain POPs in refs 25 and 26. The effect of temperature on chemical K_{OW} (represented by eq 6) has been shown to be relatively minor for most POPs (27):

$$\log K_{OW} = A_{OW} - \Delta H_{OW} / 2.303 \cdot RT \quad (6)$$

ΔH_{OW} is the enthalpy of phase transfer between octanol and water ($kJ \cdot mol^{-1}$), R is the gas constant ($J \cdot mol^{-1} \cdot K^{-1}$), and A_{OW} parameters are compound specific. The temperature dependence of K_{AW} is related to the chemical's Henry's Law constant (H , $Pa \cdot m^3 \cdot mol^{-1}$), as $K_{AW} = H/RT$. Henry's Law constants of POPs can be very sensitive to ambient temperature changes (28) and is expressed as

$$\log H = A_H - B_H/T \quad (7)$$

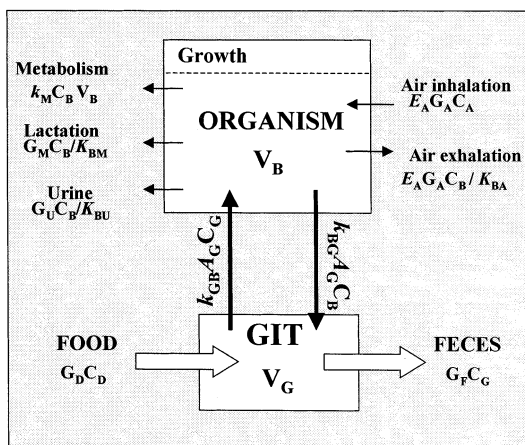


FIGURE 2. Conceptual two-compartment bioaccumulation model for terrestrial mammals showing uptake and elimination processes.

where A_H and B_H are derived for specific POPs based on ref 28.

Bioaccumulation Model for Terrestrial Mammals. Figure 2 is a conceptual diagram of a two-compartment bioaccumulation model for terrestrial mammals, consisting of a gastrointestinal tract (GIT) and an organism compartment which represents the animal's overall contaminant storage. A glossary of the terms used in the terrestrial mammal model derivation is shown in Table S-1 (see Supporting Information). The model is based on the assumption that gastrointestinal magnification is the primary mechanism driving gastrointestinal uptake and biomagnification of organic chemicals. In essence, the GIT compartment receives food at the rate of ingestion, i.e., the product of the ingestion rate G_D in $\text{m}^3 \cdot \text{h}^{-1}$ and the dietary concentration C_D ($\text{mol} \cdot \text{m}^{-3}$) or $G_D C_D$ ($\text{mol} \cdot \text{h}^{-1}$) and eliminates fecal matter at a rate of $G_F C_G$ ($\text{mol} \cdot \text{h}^{-1}$), i.e., the product of the fecal egestion rate G_F ($\text{m}^3 \cdot \text{h}^{-1}$) and the intestinal concentration C_G ($\text{mol} \cdot \text{m}^{-3}$). Diffusion at rates of $k_{GB} A_G C_G$ ($\text{mol} \cdot \text{h}^{-1}$) and $k_{BG} A_G C_B$ ($\text{mol} \cdot \text{h}^{-1}$) describe the exchange of chemical between the GIT compartment and the organism. k_{GB} and k_{BG} are the mass transfer coefficients in units of ($\text{m} \cdot \text{h}^{-1}$) for diffusion from the GIT into the organism and from the organism to the GIT, respectively, and A_G (m^2) is the area over which diffusion occurs. The net chemical flux into the GIT (N_G , $\text{mol} \cdot \text{h}^{-1}$) can be represented as

$$N_G = G_D C_D + k_{BG} A_G C_B - (G_F + k_{GB} A_G) \cdot C_G \quad (8)$$

where V_G is the volume of the intestinal tract (m^3) and t is time (h).

The degree of chemical accumulation in the organism's tissues is due to competing rates of chemical uptake, i.e., through air inhalation ($G_A E_A C_{AG}$) and absorption from the GIT ($k_{GB} A_G C_G$), and rates of chemical elimination through exhalation, i.e., ($G_A E_A C_B / K_{BA}$), urine excretion ($G_U C_B / K_{BU}$), fecal egestion ($k_{BG} A_G C_B$), milk excretion ($G_M C_B / K_{BM}$), and metabolic transformation ($k_M V_B C_B$). The mass balance equation representing the net chemical flux ($\text{mol} \cdot \text{h}^{-1}$) into the organism (N_B) is thus represented by

$$N_B = G_A E_A C_{AG} + k_{GB} A_G C_G - (G_A E_A / K_{BA} + k_{BG} A_G + G_U / K_{BU} + G_M / K_{BM} + k_M V_B) \cdot C_B \quad (9)$$

where V_B is the volume of the organism (m^3), G_A is the inhalation rate ($\text{m}^3 \cdot \text{h}^{-1}$), E_A is the inhalation efficiency (no units), and C_{AG} is the gaseous aerial concentration ($\text{mol} \cdot \text{m}^{-3}$). G_U is the urinary excretion rate ($\text{m}^3 \cdot \text{h}^{-1}$), G_M is the milk excretion rate ($\text{m}^3 \cdot \text{h}^{-1}$) for female animals, and k_M is the metabolic transformation rate constant (h^{-1}). K_{BA} , K_{BU} , and

K_{BM} are volume normalized partition coefficients (unitless) between organism and air, organism and urine, and organism and milk, respectively. Assuming continuous feeding and a steady-state condition in the GIT (i.e., $N_G = 0$) and recognizing that the gross chemical dietary uptake efficiency (E_D) in the organisms is $E_D = k_{GB} A_G / (G_F + k_{GB} A_G)$, substitution of eq 8 into 9 gives

$$N_B = G_{AG} E_A C_{AG} + G_D E_D C_D - (G_A E_A / K_{BA} + (E_D / K_{BG}) G_F + G_U / K_{BU} + G_M / K_{BM} + k_M V_B) C_B \quad (10)$$

The model estimates an age dependent biomagnification factor for terrestrial organisms as N_B is $d(V_B C_B) / dt$, providing an estimate of C_B as a function of time. Following observations in refs 29 and 30, concentrations in the fetus are assumed to be at equilibrium with those in the pregnant female. This model identifies lipid-to-air partitioning (K_{BA}) and gastrointestinal magnification ($K_{DG} = G_D / G_F$) as the main driving forces for bioaccumulation of POPs, while urinary excretion, milk excretion, metabolic transformation, and growth dilution counteract the bioaccumulation process. Biomagnification in the model occurs as a result of food digestion which (i) reduces the fecal egestion rate G_F below the dietary ingestion rate G_D and (ii) elevates the biota-to-GIT partition coefficient K_{BG} above the biota-to-diet partition coefficient K_{BD} . Elimination through air-exhalation, urine, milk, and metabolic transformation combine to reduce the degree of biomagnification achieved by dietary absorption and digestion. Changes in the organism's biomass, which is particularly important for nursing newborns and fasting animals, is presented in the model as the time dependence of the weight of the animal, i.e., dV_B / dt in this time dependent model. It acts to reduce biomagnification during periods of growth (growth dilution) and increase biomagnification during periods of biomass loss (e.g. winters). The model assumes that for continuously exposed animals in the field, concentrations of POPs among different tissues are at a chemical equilibrium and hence are homogeneously distributed within the animal when expressed on a lipid normalized basis. Field observations (17) and analyses using physiologically based pharmacokinetic (PBPK) models (31) support this simplification for certain animals, including those used in this study.

In terms of organic chemical partitioning, the organism is viewed as consisting of three phases: (i) lipid, (ii) nonlipid organic matter such as proteins, and (iii) water. Assuming that phase properties of lipids are adequately represented by octanol and that nonlipid organic matter (i.e. all organic matter excluding the lipids) has a sorption affinity equal to 3.5% of that of octanol, the biota-to air partition coefficient K_{BA} can be estimated as

$$K_{BA} = C_B / C_{AG} = \nu_{LB} K_{OA} + 0.035 \cdot \nu_{NB} K_{OA} + \nu_{WB} / K_{AW} \quad (11)$$

where ν_{LB} , ν_{NB} , and ν_{WB} are respectively the lipid content (kg lipid/kg wet wt organism), the nonlipid organic matter content (kg nonlipid organic matter/kg wet wt organism), and the water content (kg water/kg wet wt organism) of the predator organism. Partition coefficients for octanol-air (K_{OA}) and air-water (K_{AW}) are temperature corrected for internal body temperature ($\sim 37^\circ \text{C}$) and are thus different from those values of K_{OA} and K_{AW} calculated at ambient temperatures in the vegetation model.

Following the same three-phase partitioning model for intestinal contents, the organism-to-GIT partition coefficient K_{BG} can be derived as

$$K_{BG} = C_B / C_G = (\nu_{LB} + 0.035 \cdot \nu_{NB} + \nu_{WB} / K_{OW}) / (\nu_{LG} + 0.035 \cdot \nu_{NG} + \nu_{WG} / K_{OW}) \quad (12)$$

where ν_{LG} , ν_{NLOMG} , and ν_{WG} are respectively the lipid content

(kg lipid/kg wet wt digesta), the nonlipid organic matter content (kg nonlipid organic matter/kg wet wt digesta), and the water content (kg water/kg wet wt digesta) of the intestinal content and $\nu_{LG} + \nu_{NG} + \nu_{WG} = 1$. They are dependent on the digestibility of the ingested diet, which can be expressed by the absorption efficiencies of lipid (ϵ_L), nonlipid organic matter (ϵ_N), and water (ϵ_W) according to

$$\nu_{LG} = (1 - \epsilon_L) \cdot \nu_{LD} / \{ (1 - \epsilon_L) \cdot \nu_{LD} + (1 - \epsilon_N) \cdot \nu_{ND} + (1 - \epsilon_W) \cdot \nu_{WD} \} \quad (13)$$

$$\nu_{NG} = (1 - \epsilon_N) \cdot \nu_{ND} / \{ (1 - \epsilon_L) \cdot \nu_{LD} + (1 - \epsilon_N) \cdot \nu_{ND} + (1 - \epsilon_W) \cdot \nu_{WD} \} \quad (14)$$

$$\nu_{WG} = (1 - \epsilon_W) \cdot \nu_{WD} / \{ (1 - \epsilon_L) \cdot \nu_{LD} + (1 - \epsilon_N) \cdot \nu_{ND} + (1 - \epsilon_W) \cdot \nu_{WD} \} \quad (15)$$

where ν_{LD} , ν_{ND} , and ν_{WD} are the lipid content (kg lipid/kg wet weight food), the nonlipid organic matter content (kg nonlipid organic matter/kg wet wt food), and the water content (kg water/kg wet wt food) of the ingested diet. The organism to urine partition coefficient K_{BU} and organism to milk partition coefficient (K_{BM}) are derived from K_{OW} and represented as

$$K_{BU} = (\nu_{LB} + 0.035 \cdot \nu_{NB}) K_{OW} + \nu_{WB} \quad (16)$$

$$K_{BM} = \{ (\nu_{LB} + 0.035 \cdot \nu_{NB}) K_{OW} + \nu_{WB} \} / \{ (\nu_{LM} + 0.035 \cdot \nu_{NM}) K_{OW} + \nu_{WM} \} \quad (17)$$

where ν_{LM} is the lipid content of the milk, ν_{NM} is the nonlipid organic matter content of the milk, and ν_{WM} is the water content of the milk.

Model Parametrization and Application

Chemical Properties. A summary of the relevant chemical properties of the 25 organic compounds studied is shown in Table S-2 (see Supporting Information). Vapor pressures, K_{OWs} , K_{OAS} , and H values are temperature corrected and are comparable to reported values in the literature (21, 22, 25, 27, 32–34). Following Boon et al. (35), PCB congeners were categorized into four groups of metabolic transformation potential on the basis of known metabolism in mammalian species by P450 enzymes.

Atmospheric Variables. The monthly ambient air temperature profile was derived from ref 36 and ranges from approximately -30 °C in January to approximately 20 °C in July. Measured values of θ in Arctic air are approximately 1×10^{-6} (October to April) and 1×10^{-7} $\text{cm}^2 \cdot \text{cm}^{-3}$ (May to September), respectively (16).

Lichen. Values of A_V/V_V range between 3000 and 10 000 for $\text{m}^2 \cdot \text{m}^{-3}$ for vascular plants (37) and was approximated to be 10^6 $\text{m}^2 \cdot \text{m}^{-3}$ for lichens and 10^4 $\text{m}^2 \cdot \text{m}^{-3}$ for willows. The lipid content was 0.5% and 1% for lichens and willows, respectively, and the nonlipid organic matter content was 40% and 30%, respectively (17). δ_G was $5 \text{ m} \cdot \text{h}^{-1}$ and δ_P was $3 \text{ m} \cdot \text{h}^{-1}$ (38, 39). During winter months δ_G was reduced to $0.5 \text{ m} \cdot \text{h}^{-1}$ due to the overlying snowpack. δ_W was estimated from surface water runoff at approximately $1 \times 10^{-4} \text{ m} \cdot \text{h}^{-1}$ (39–41), and k_E was approximated as 0.002 h^{-1} based on ref 12. The temperature of the lichens is lowest (i.e., -20 °C) in November (assuming no snow cover) and -2 °C from December through April assuming lichens are insulated under the snowpack.

Mammals. From ref 42, the resting lung ventilation rates (G_A , $\text{m}^3 \cdot \text{h}^{-1}$) for caribou and wolves were estimated from an allometric relationship with the animal's body size (V , m^3):

$$G_A (\text{m}^3 \text{ h}^{-1}) = 3.6 (V)^{0.75} \quad (18)$$

Following ref 31 we assume approximately 70% of alveolar air is assumed to achieve an equilibrium with arterial blood, while the remaining 30% is poorly mixed. Consequently, a 70% assimilation efficiency of inhaled air (i.e., $E_A = 0.7$) is applied to eq 11. The effective resting ventilation rates ($E_A G_A$) for adult barren-ground caribou and wolves are approximately $18 \text{ m}^3 \cdot \text{d}^{-1}$ and $13 \text{ m}^3 \cdot \text{d}^{-1}$, respectively.

Caribou graze primarily on lichens but also feed on willow leaves during late summer (43). From previous observations (44) the wolf diet (assumed as 100% caribou) is comprised of 70% adult caribou, 20% caribou calves, and 10% caribou yearlings. Feedings rates are $3.0 \pm 1.5 \text{ kg} \cdot \text{d}^{-1}$ dry wt for caribou (43) and $2.5 \pm 1.0 \text{ kg} \cdot \text{d}^{-1}$ wet wt for wolves (44, 45). The dietary uptake efficiency E_D tends to decline for chemicals with $\log K_{OWs}$ exceeding 7. For example, E_D values of various compounds over a $\log K_{OW}$ range of 5.0–8.0, decreased from 80% to 15% in dairy cows (46) and from 98% to 70% in humans (47, 48). For the purpose of this study, K_{OW} - E_D relationship for caribou and wolves is assumed to be comparable to those observations in dairy cows and humans, respectively. Both caribou and wolves exhibit large growth fluctuations and changes in fat contents throughout the year (43–45, 49, 50). Temporal changes in ingesta free-body lipid content (% lipid) and lifetime growth profiles (kg) for male caribou and wolves are shown in Figure S-1 (see Supporting Information). Maximum body weights for adult male caribou and wolves are approximately 140 and 80 kg, respectively. Ingesta-free body fat for caribou range from approximately 4% (spring) to 25% (fall) and approximately 7% (spring) to 21% (fall) for wolves. For caribou, the lipid extraction efficiency was set at 65%, and the nonlipid organic matter extraction efficiency at 50%. The water extraction efficiency is set to 95%, which results in 50% water in the digesta. This produces a 60% food absorption (in agreement with 51) and hence a G_D/G_F ratio of 2.5, a diet-to-GIT (K_{DG}) partition coefficient of 0.8, and an overall gastrointestinal magnification factor of 2.5×0.8 or 2.0. For wolves, the lipid extraction efficiency was set at 99%, the nonlipid organic matter extraction efficiency was set at 70%, and the water extraction efficiency was 95%. This results in 95% food absorption (in agreement with ref 51), a G_D/G_F ratio of 20, a K_{DG} of 7, and an overall gastrointestinal magnification factor $K_{DG} \cdot G_D/G_F$ of approximately 140. A summary of the values and sources of the various model parameters are shown in Table S-3 (see Supporting Information).

Model Application. Measured concentrations of the 25 organic chemicals in Arctic air (15, 36, 52, 53) and snowpack meltwater (36, 54) were used as input parameters to generate hourly concentrations (i.e., $dt = 1 \text{ h}$) in lichens, willows, caribou, and wolves. Freely dissolved chemical concentrations in snowpack meltwater (C_{WD} , $\text{mol} \cdot \text{m}^{-3}$ meltwater) were determined from total concentrations observed in snowpack meltwater (C_{SP} , $\text{mol} \cdot \text{m}^{-3}$ meltwater) and estimated dissolved fractions in meltwater (ϕ_{WD}) using the equation $C_{WD} = \phi_{WD} \cdot C_{SP}$. Typical values of ϕ_{WD} for hydrophobic compounds such as chlorobenzenes and PCBs range between 15% and 40% (55).

Simulations were conducted for (i) male and female caribou and (ii) male and female wolves, generating hourly chemical concentrations ($\text{ng} \cdot \text{g}^{-1}$ lipid) in those individual animals. At the time of parturition for caribou ($t_0 = \text{June}$) and wolves ($t_0 = \text{May}$), the neonate was assigned a lipid equivalent concentration equal to that of the pregnant female. Postparturition, maternal milk is ingested by the neonate over a specified nursing period. Lipid normalized chemical concentrations in milk (C_M , $\text{mol} \cdot \text{m}^3$ lipid) are assumed to equal those concentrations in the adult female's tissues' (i.e., $C_M = C_B$), based on previous observations of an internal chemical equilibrium for caribou and wolves (17). Monte Carlo simulations (MCS) with sample sizes of 10 000 were

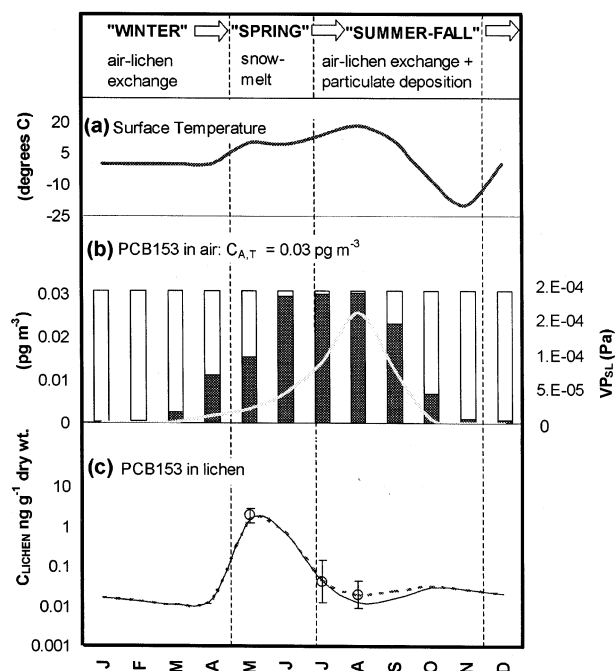


FIGURE 3. Illustration of (a) monthly air temperature ($^{\circ}\text{C}$), (b) vapor pressure (VP_{SL}) and atmospheric phase distribution of PCB153, and (c) PCB153 concentrations in lichen ($\text{ng}\cdot\text{g}^{-1}$ dry wt). In plot (b) gas-phase and particulate-phase concentrations in air are shown as solid bars and white bars, respectively, and the gray line represents VP_{SL} of PCB 153. In plot (c) lichen concentrations due solely to gas-phase partitioning (C_{VG}) is solid line, while total concentrations including particulate-bound accumulation (i.e., $C_{\text{VT}} = C_{\text{VG}} + C_{\text{VP}}$) is a dashed line. Data points in plot (c) are geometric means and standard deviations of PCB153 measured in the lichen *Cl. rangiferina* sampled near Bathurst Inlet during May, July, and August (17).

conducted using Crystal Ball © (Decisioneering) to report measures of uncertainty associated with variability in model input parameters. The mean and standard deviations of input parameters were used in the MCS to calculate 95% confidence intervals of the predicted concentrations. To assess the predictability of the model, predicted concentrations (C_{p}) in caribou and wolf tissues ($\text{ng}\cdot\text{g}^{-1}$ lipid) were compared to the observed concentrations (C_{o}) in animals sampled from Cambridge Bay, Bathurst Inlet, and Inuvik (17).

Results and Discussion

Bioaccumulation in Lichens. Figure 3 illustrates the seasonal changes in ground surface temperature (3a) and its net effect on the vapor pressure and atmospheric phase distribution of PCB153 (3b) and predicted PCB153 dry wt concentrations in lichens (3c). Observed PCB 153 concentrations in lichens (*Cl. rangiferina*) from ref 17 are shown for comparison. For PCB153 the change in VP_{SL} from 1.8×10^{-4} Pa in summer (20°C) to 1.0×10^{-7} Pa in winter (-30°C) causes the fraction of the total atmospheric concentration in gaseous form to increase from approximately 1% in January to approximately 98% in August. Assuming a constant total aerial concentration for PCB 153 of $0.03 \text{ pg}\cdot\text{m}^{-3}$, the gas-phase concentration of PCB 153 (C_{G}) increases from $2.6 \times 10^{-4} \text{ pg}\cdot\text{m}^{-3}$ in January to $0.029 \text{ pg}\cdot\text{m}^{-3}$ in August. During winter months (December to April) lichens are typically covered by an overlying snowpack (lichen surface temp = -2°C) and are exposed primarily to POPs through gaseous concentrations. K_{VG} (i.e., $C_{\text{V}}/C_{\text{G}}$) is relatively large during this cold period. During spring snowmelt ($\sim 10\text{--}15$ days, late May) exposure to meltwater provides an important route of uptake in lichens. Concentrations of POPs in meltwater can be relatively high compared

to air because of extensive accumulation of POPs in the snowpack over the winter (36, 52). Figure 3 shows that highest concentrations of PCB153 can be expected in the spring as lichens attempt to reach an equilibrium with the snowpack meltwater. Concentrations of PCB153 in arctic snowpack were approximately $0.15 \text{ ng}\cdot\text{L}^{-1}$ meltwater (36, 52, 54). After the snowmelt has subsided, temperatures rise and concentrations in lichens approach a new equilibrium with the relatively lower gaseous concentrations in the air during summer months (K_{VG} is relatively small during this warm period).

During summer months vegetation can accumulate chemical through both gas-phase partitioning and particulate deposition. Figure 3 shows total PCB153 lichen concentrations during this period are due to a combination of gas-phase partitioning (64%) and particulate deposition (36%). In contrast, concentrations of relatively more volatile POPs such as hexachlorobenzene in lichens during summer are entirely due to gas-phase partitioning (see Figure S-2, Supporting Information). Gas-phase partitioning is predominant for substances such as chlorobenzenes and HCHs that exhibit K_{OAS} between 10^6 and 10^{11} , while the particulate-bound chemical contribution to vegetation concentrations becomes significant if K_{OA} exceeds 10^{11} (12). The significance of Figure 3 is that (i) concentrations of POPs in lichens are highest during the spring when terrestrial mammals have depleted fat reserves and are producing offspring, (ii) POPs concentrations are lowest during summer and fall months when terrestrial mammals are actively feeding and storing winter fat reserves, and (iii) temperature is an important determinant of vegetation concentrations due to its influence on atmospheric phase distribution and the vegetation-air partition coefficient, K_{VG} . Model predicted concentrations of POPs in lichens were in general agreement with the observed data (17).

Bioaccumulation in Caribou and Wolves. Figure 4 illustrates model predicted tissue concentrations ($\text{ng}\cdot\text{g}^{-1}$ lipid) of PCB 153 over a 14 year life-span for (a) male caribou, (b) female caribou, (c) male wolves, and (d) female wolves from Bathurst Inlet. Observed data for individual animals sampled near Bathurst Inlet are shown for comparison. Post-parturition, caribou calves ($t_0 = \text{June}$) and wolf pups ($t_0 = \text{May}$) are shown to experience only slight increases in tissue concentrations following maternal transfer, due primarily to the newborn's rapid growth rate which provides a dilution effect during this sensitive life-stage. The successive cyclical fluctuations of tissue concentrations are primarily due to a combination of seasonal changes in lipid content and body size and/or milk excretion for female animals. While the 10–100-fold increase in concentrations in lichens during spring following spring melt event (Figure 3) has a significant effect on the actual magnitude of POPs concentrations in caribou and wolves, it is important to recognize that the effect of physiological changes in these animals is a more important factor causing the increase in concentrations (Figure 4). Specifically, growth and increasing lipid contents during the fall causes a dilution of chemical residues in the animal's tissues, resulting in a reduction in tissue concentrations. Fat depletion during spring concentrates chemical residues, causing a rise in concentrations in the animal's tissues. For mature female animals (2+ years), tissue concentrations decline sharply during spring, corresponding to periodic elimination via lactation throughout the nursing period. The model reasonably predicts (i) the seven times increase in PCB 153 male caribou tissue concentrations between September and July and (ii) the lower concentrations in female animals compared to males (17). In general, observed PCB 153 concentrations are comparable to the model predicted concentrations and consistently fall within the model uncertainty determined by MCS. This indicates that variability

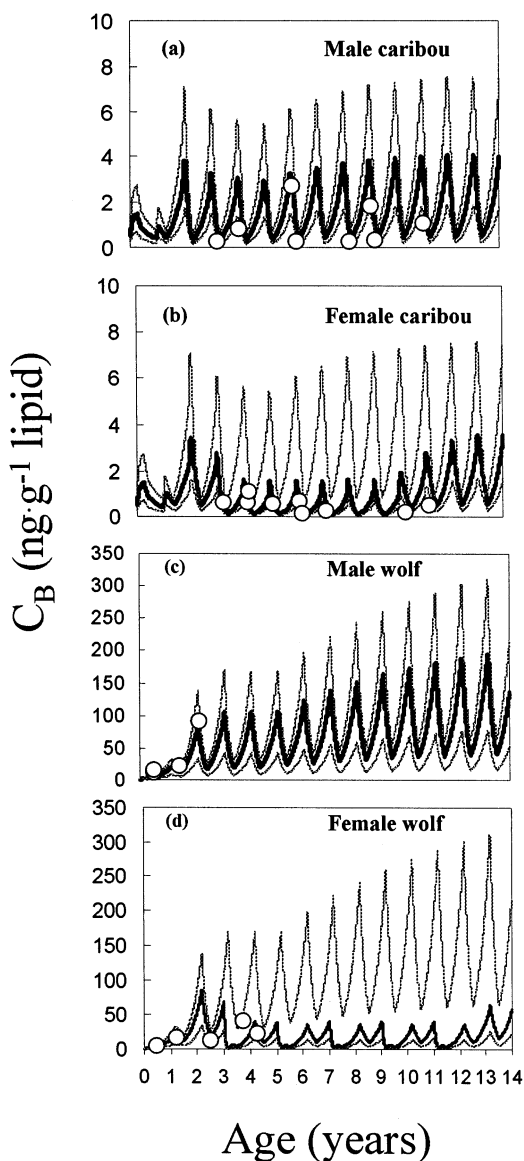


FIGURE 4. Predicted chemical concentrations ($\text{ng}\cdot\text{g}^{-1}$ lipid) in the tissues of (a) male caribou, (b) female caribou, (c) male wolves, and (d) female wolves from Bathurst Inlet over a 14-year life-span. Data points represent measured concentrations of PCB153 in fat tissue of individual caribou and wolves from Bathurst Inlet (17). Lines above and below predicted value represent upper and lower 95% confidence intervals, calculated using Monte Carlo simulation.

in the model input parameters can account for differences between observed and predicted concentrations. Figure 5 illustrates several plots comparing observed and model predicted concentrations (i.e., $\log C_O$ vs $\log C_P$) of various organic contaminants in caribou and wolves from Bathurst Inlet. HCB and HCH concentrations are shown to be greater than those of the various PCB congeners and other organochlorine compounds. The majority of the observed data (C_O) are in general agreement with model predicted concentrations (C_P) and predominantly lie within calculated upper and lower 95% confidence intervals of the predicted concentrations. Similar plots of observed versus predicted concentrations in caribou and wolves for model simulations of lichen-caribou-wolf food-chains at Cambridge Bay and Inuvik are shown in Figure S-3 (see Supporting Information).

Food-Chain Bioaccumulation. Model predicted bioaccumulation factors (BAFs) of the various organic chemicals in lichens (C_{VT}/C_{AG}) and caribou and wolves (C_B/C_{AC}) increase

with increasing chemical K_{OA} (Figure 6). Specifically, BAFs increase between 10^5 and 10^{12} for lichens and from 10^5 and 10^{15} for caribou and wolves (over a K_{OA} range of 10^5 – 10^{12}). The predicted linear increase of the BAF for lichens with increasing K_{OA} is consistent with previous BAF- K_{OA} relationships reported for vascular plants (23) and lichens (56) for POPs with K_{OA} between 10^5 and 10^{11} . For compounds with $K_{OA} > 10^{12}$, particulate-bound deposition becomes a more significant factor affecting air-to-vegetation contaminant transfer and the resulting BAF. Because the chemicals examined in the present study all exhibit K_{OAS} between approximately 10^5 and 10^{12} the BAFs presented for lichens are primarily a function of the equilibrium distribution of chemical in the gas-phase and vegetation (i.e., K_{VG}). Also, the BAF shown in Figure 6 relates the vegetation concentration to the gaseous aerial concentration and is hence independent of the particulate bound fraction. It is important to note that observations in vascular plants (23, 57) indicate that plant materials can vary significantly in their partitioning properties due to differences in sorptive capacity and that colder ambient air temperature causes an increase in K_{VG} due to the temperature dependence of chemical K_{OA} (eq 5). Thus, surface temperature and the sorptive capacity of a given vegetation species significantly influence equilibrium concentrations in vegetation which ultimately affects the BAFs for terrestrial mammals.

The predicted BAFs for caribou and wolves increase substantially with increasing K_{OA} . For example, relatively “low” K_{OA} chemicals (i.e., $K_{OA} < 5$) exhibit BAFs for caribou and wolves between approximately 10^3 and 10^5 . In contrast, relatively “high” K_{OA} chemicals ($\log K_{OA} \sim 11$) are shown to exhibit BAFs ranging from approximately 10^{11} for adult female caribou to 10^{13} for adult male wolves. The model predicted BAFs for caribou and wolves depicted in Figure 6 are comparable to observed BAFs based on available atmospheric and biological monitoring data (15, 17, 52, 53). This is confirmed by the relatively good model agreement with measured concentrations. In terms of chemical bioaccumulation in terrestrial wildlife, the significance of the predicted BAFs presented is 2-fold: (i) lower BAFs for females compared to males is the result of maternal transfer of contaminant and (ii) the stepwise increase in BAFs and hence lipid normalized chemical concentration with increasing trophic level highlights the importance of dietary exposure and biomagnification for chemical bioaccumulation in this terrestrial food-chain.

Male wolves represent the most susceptible biological endpoint for the accumulation of substances that can biomagnify due to (i) their top-predator position in this terrestrial food-chain and (ii) their inability to eliminate chemical via maternal transfer. A summary of biomagnification factors (BMFs) of various organic chemicals (ordered by increasing hydrophobicity) predicted by the model for male wolves at 1.5 years (winter), 2.25 years (late summer), and 13.1 years (spring) is shown in Table 1. The listed compounds, which include several PCB congeners, pesticides, and two hypothetical chemicals, are wide ranging in K_{OW} and K_{OA} . First, temporal factors (i.e., age and season) are shown to influence the BMFs of individual male wolves. Specifically, older males during spring (e.g., 13.1 years old) are shown to exhibit the greatest BMFs due to (i) a greater lifetime of contaminant exposure and (ii) reduced fat reserves during spring compared to late summer and winter months. For example, the BMF for PCB 206 for male wolves at 1.5, 2.25, and 13.1 years of age are 18.9, 64.9 and 165.5, respectively. Second, the magnitude of the BMFs for individual wolves of a given age does not appear to be related to the chemical’s hydrophobicity. In some cases, relatively hydrophilic compounds such as β -endosulfan and β -HCH ($\log K_{OW} < 4$) exhibit greater BMFs than more hydrophobic

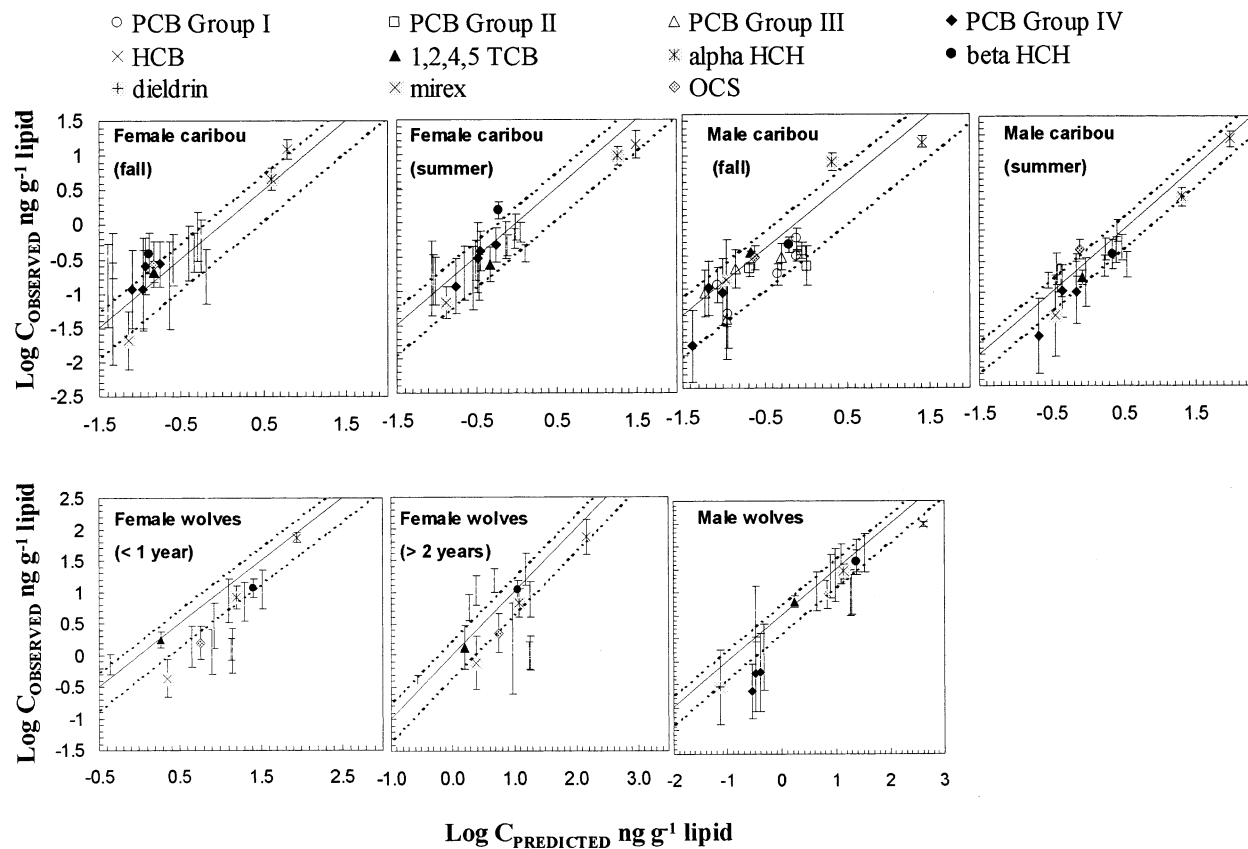


FIGURE 5. Observed versus predicted chemical concentrations (i.e., $\log C_O$ vs $\log C_P$) in ng g^{-1} lipid of various organic contaminants for caribou and wolves from Bathurst Inlet. Data points and error bars represent logarithms of the geometric mean (GM) and standard deviation of the GM, respectively. The solid line represents perfect model agreement. Dashed lines represent 95% confidence intervals of predicted concentrations, calculated using Monte Carlo simulation.

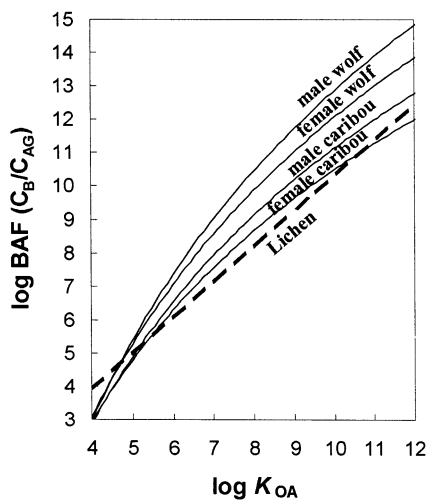


FIGURE 6. Model predicted bioaccumulation factors (presented as $\log \text{BAF}$) for lichens, caribou (males and females), and wolves (males and females) versus $\log K_{OA}$ of various organic chemicals (ranging in $\log K_{OA}$ between 4 and 12). BAFs for caribou and wolves are represented by ratio of the chemical concentration in the animal's tissues' (C_B , $\text{mol} \cdot \text{m}^{-3}$ lipid) and the gas-phase concentration in ambient air (C_{AG} , $\text{mol} \cdot \text{m}^{-3}$), (i.e., $\text{BAF} = C_B/C_{AG}$). BAFs for lichens are represented by the ratio of the chemical concentration in the lichens (C_{VT} , $\text{mol} \cdot \text{m}^{-3}$ equivalent lipid) and the gas-phase air concentration (i.e., $\text{BAF} = C_{VT}/C_{AG}$).

compounds such as HCB ($\log K_{OW} = 5.5$). The model indicates that these relatively hydrophilic and nonmetabolizable chemicals biomagnify in terrestrial mammals due to their

TABLE 1. Predicted BMFs (kg lipid/kg lipid), i.e. (C_B/C_D) in Wolves for Various Organic Chemicals Ranging in K_{OW} and K_{OA}

compound	$\log K_{OW}$ (20 °C)	$\log K_{OA}$ (20 °C)	BMF male wolf		
			1.5 years old	2.25 years old	13.1 years old
chemical X (hypothetical)	1.2	7.0	0.9	0.3	0.5
chemical Y (hypothetical)	3.5	5.0	0.1	0.6	0.5
β -endosulfan	3.7	7.2	5.3	17.9	39.8
β -HCH	3.8	8.1	9.1	28.8	108.5
1,2,4,5 TCB	4.6	5.8	3.2	4.1	4.9
HCB	5.5	7.1	5.4	18.6	41.1
PCB 153	6.9	9.8	18.1	63.9	157.9
PCB 180	7.4	10.7	18.8	64.6	163.3
PCB 206	8.1	11.2	18.9	64.9	165.5

relatively high K_{OAS} ($\log K_{OAS} > 6.0$) and hence negligible respiratory elimination.

Figure 7 illustrates predicted and observed BMFs of various organic chemicals for male wolves at Bathurst Inlet in relation to the chemical's octanol-air partition coefficient ($\log K_{OA}$ ranges between 4 and 10). The effect of age is also evident from this plot. Figure 7 illustrates that BMFs in wolves increase with increasing K_{OA} . The relationship between the BMF and K_{OA} is due to the fact that a high degree of gastrointestinal uptake is counter balanced by elimination through exhalation to the air. For substances with a relatively low K_{OA} exhalation is an effective route of elimination, resulting in a relatively low BMF. But when K_{OA} rises, exhalation becomes an increasingly less significant route of elimination. This causes the internal concentrations in the wolves to approach those in their gastrointestinal system and produce a high degree

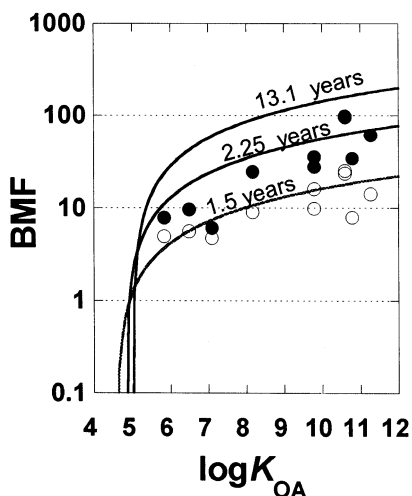


FIGURE 7. Predicted and observed BMFs (log scale) for male wolves from Bathurst Inlet versus the chemical's $\log K_{OA}$. Model predictions (solid lines) represent BMFs in male wolves 1.5, 2.25, and 13.1 years of age. Dark circles represent observed BMFs in Bathurst male wolves (2.25 years of age), and white circles represent observed BMFs in 1.5 year-old male wolves from Bathurst Inlet (17). No chemical concentration data exist for older wolves (i.e., > 4 years).

of biomagnification. The predicted BMF- K_{OA} relationships presented in Figure 7 suggest nonmetabolizable chemicals with K_{OAS} less than approximately 10^5 do not biomagnify in this food-chain. This is further illustrated by the forecasted BMFs of the relatively "low" K_{OA} compounds in Table 1. The simulation of 1,2,4,5 TCB ($\log K_{OA} = 5.8$) elicits BMFs slightly greater than 1.0 in male wolves (i.e., approximately 2–4), and forecasted BMFs of a hypothetical compound denoted as "Chemical Y" ($\log K_{OW} = 3.5$; $\log K_{OA} = 5.0$) are less than or approximately equal to 1.0. Forecasted BMFs in caribou also indicate that chemicals with $K_{OAS} < 10^5$ do not biomagnify (i.e., $BMF < 1$) due to efficient elimination of those compounds via air-exhalation.

The model calculations further illustrate that "high" K_{OA} compounds that are relatively hydrophilic (i.e., $\log K_{OW} \leq 2$) exhibit a reduced gastrointestinal uptake and efficient excretion in urine. This reduces the chemical's biomagnification potential. This effect is illustrated by the forecasted BMFs of a relatively hydrophilic yet relatively nonvolatile compound X ($\log K_{OW} = 1.2$; $\log K_{OA} = 7.0$) in Table 1. The biomagnification potential of very hydrophobic compounds may also be reduced by slower GIT-to-organism partitioning and hence increased fecal elimination of those compounds. Also, significant chemical degradation in the environment (e.g., photolysis) and metabolism of some organic compounds can effectively reduce or eliminate (i) chemical exposure and/or (ii) internal tissue concentrations, thereby diminishing the chemical's biomagnification potential, regardless of the chemical's K_{OA} or K_{OW} .

Currently, toxic substance management policies and supporting legislation are based on observations in aquatic systems and generally identify "bioaccumulative" substances as those substances with $K_{OWS} > 10^5$. Our study shows that the fundamental principles inherent to current management policies do not correctly identify the bioaccumulation potential of organic chemicals in terrestrial mammals and possibly humans and other various air-breathing animals. We propose that current regulatory initiatives aimed to identify bioaccumulative substances recognize the fundamental difference in the bioaccumulation mechanism between "air-breathing" and "water-ventilating" organisms. This can be accomplished by including K_{OA} as a bioaccumulation predictor in addition to K_{OW} . Our study indicates

that substances with a $\log K_{OA} > 5$ and a $\log K_{OW} > 2$ have an inherent biomagnification potential in certain terrestrial food-chains. However, sufficiently high chemical and/or metabolic transformation rates as well as physiological factors (e.g. lactation, growth) can produce actual biomagnification factors that are less than expected from the chemical's inherent biomagnification potential either for specific periods of time or in perpetuity. We hope that the model developed in this study will be helpful in understanding and assessing the bioaccumulation potential of commercial chemicals in terrestrial food-chains and prevent the accumulation of potentially toxic substances in terrestrial food-chains in the future.

Acknowledgments

We thank Dr. William Strachan and Jon Arnot and acknowledge the financial support of the Natural Sciences and Engineering Research Council of Canada, the Association of Canadian Universities for Northern Studies.

Supporting Information Available

Tables S-1, S-2, and S-3 and Figures S-1, S-2, and S-3. This material is available free of charge via the Internet at <http://pubs.acs.org>.

Literature Cited

- Gobas, F. A. P. C. *Ecological Modelling* **1993**, *69*, 1.
- Morrison, H. A.; Gobas, F. A. P. C.; Lazar, R.; Whittle, M.; Haffner, G. D. *Environ. Sci. Technol.* **1997**, *31*, 3267.
- USEPA. *Great Lakes Water Quality Initiative Technical Support Document to determine Bioaccumulation Factors*; Report No. 822-R-94-002; 1994.
- McLachlan, M. S. *Environ. Sci. Technol.* **1996**, *30*, 252.
- Thomas, D. J.; Tracey, B.; Marshall, H.; Norstrom, R. J. *Sci. Total Environ.* **1992**, *122*, 135.
- Landers, D. H.; Bangay, G.; Sisula, H.; Colborn, T.; Liljelund, L. E. *Sci. Total Environ.* **1995**, *160*, 841.
- Sharpe, S.; Mackay, D. *Environ. Sci. Technol.* **2000**, *34*, 2373.
- Tolls, J.; McLachlan, M. S. *Environ. Sci. Technol.* **1994**, *28*.
- McLachlan, M. S.; Welsch-Pausch, K.; Tolls, J. *Environ. Sci. Technol.* **1995**, *29*, 1998.
- Riederer, M. *Environ. Sci. Technol.* **1990**, *24*, 829.
- Paterson, S.; Mackay, D.; Bacci, E.; Calamari, D. *Environ. Sci. Technol.* **1991**, *25*, 866.
- McLachlan, M. S. *Environ. Sci. Technol.* **1999**, *33*, 1799.
- Carlberg, G. E.; Baumann-Ofstad, E.; Drangsholt, H. *Chemosphere* **1983**, *12*, 341.
- Villeneuve, J. P.; Fogelqvist, E.; Cattini, C. *Chemosphere* **1988**, *17*, 399.
- Stern, G. A.; Halsall, C. J.; Barrie, L. A.; Muir, D. C. G.; Fellin, P.; Rosenberg, B.; Rovinsky, F. Y.; Konovov, E. Y.; Pastuhov, B. *Environ. Sci. Technol.* **1997**, *31*, 3619.
- Macdonald, R. W.; Barrie, L. A.; Bidleman, T. F.; Diamond, M. L.; Gregor, D. J.; Semkin, R. G.; Strachan, W. M. J.; Li, Y. F.; Wania, F.; Alaea, M.; Alexeeva, L. B.; Backus, S. M.; Bailey, R.; Bewers, J. M.; Gobeil, C.; Halsall, C. J.; Harner, T.; Hoff, J. T.; Jantunen, L. M. M.; Lockhart, W. L.; Mackay, D.; Muir, D. C. G.; Pudykiewicz, J.; Reimer, K. J.; Smith, J. N.; Stern, G. A.; Schroeder, W. H.; Wagemann, R.; Yunker, M. B. *Sci. Total Environ.* **2000**, *254*, 93.
- Kelly, B. C.; Gobas, F. A. P. C. *Environ. Sci. Technol.* **2001**, *35*, 325.
- Cotham, W. E.; Bidleman, T. F. *Chemosphere* **1991**, *22*, 165.
- Franz, T. P.; Eisenreich, S. J. *Environ. Sci. Technol.* **1998**, *32*, 1771.
- Wania, F.; Mackay, D.; Hoff, J. T. *Environ. Sci. Technol.* **1998**, *33*, 195.
- Falconer, R. L.; Bidleman, T. F. *Atmos. Environ.* **1994**, *28*, 547.
- Hinckley, D. A.; Bidleman, T. F.; Foreman, W. T. *J. Chem. Eng. Data* **1990**, *35*, 232.
- Komp, P.; McLachlan, M. S. *Environ. Sci. Technol.* **1997**, *31*, 2944.
- Gobas, F. A. P. C.; Wilcockson, J. B.; Russel, R. W.; Haffner, G. D. *Environ. Sci. Technol.* **1999**, *33*, 133.
- Harner, T.; Mackay, D. *Environ. Sci. Technol.* **1995**, *29*, 1599.
- Harner, T.; Bidleman, T. F. *J. Chem. Eng. Data* **1996**, *41*, 895.

- (27) Lei, Y.; Wania, F.; Shiu, W.; Boocock, D. G. B. *J. Chem. Eng. Data* **2000**, *45*, 738.
- (28) Nirmalakhandan, N.; Brennan, R. A.; Speece, R. E. *Water Res.* **1997**, *31*, 1471.
- (29) Gobas, F. A. P. C.; McCorquodale, J. R.; Haffner, G. D. *Environ. Toxicol. Chem.* **1993**, *12*, 567.
- (30) Borrell, A.; Bloch, D.; Desportes, G. *Environ. Pollut.* **1995**, *88*, 283.
- (31) Hickie, B. E.; Mackay, D.; de Koning, J. *Environ. Toxicol. Chem.* **1999**, *18*, 2622.
- (32) Hawker, D. W.; Connell, D. W. *Environ. Sci. Technol.* **1988**, *22*, 382.
- (33) Dunnivant, F. M.; Elzerman, A. W. *Environ. Sci. Technol.* **1992**, *26*, 1567.
- (34) Mackay, D.; Shui, W. Y.; Ma, K. C. *Illustrated handbook of physical-chemical properties and environmental fate of organic chemicals*; Lewis Publishers: Chelsea, MI, 1992.
- (35) Boon, J. P.; van der Meer, J.; Allchin, C. R.; Law, R. J.; Klungsoyr, J.; Leonards, P. E. G.; Spliid, H.; Storr-Hansen, E.; Mackenzie, C.; Wells, D. E. *Arch. Environ. Contam. Toxicol.* **1997**, *33*, 298.
- (36) Bidleman, T. F.; Muir, D. C. G.; Stern, G. A. *Synopsis of Research Conducted under the 1998/1999 Northern Contaminants Program*; 1999.
- (37) Trapp, S.; McFarlane, C. *Plant Contamination: Modelling and Simulation of Organic Chemical Processes*; Lewis Publishers: Boca Raton, 1995.
- (38) Horstmann, M.; McLachlan, M. S. *Atmos. Environ.* **1998**, *32*, 1799.
- (39) Mackay, D. *Multimedia Environmental Fate Models: The Fugacity Approach*; Lewis Publications: Chelsea, MI, 1991.
- (40) Di Guardo, A.; Calamari, D.; Zanin, G.; Consalter, A.; Mackay, D. *Chemosphere* **1994**, *28*, 511.
- (41) Wania, F.; Semkin, R.; Hoff, J. T.; Mackay, D. *Hydrological Proc.* **1999**, *13*, 2245.
- (42) Peters, R. H. *The Ecological Implications of Body Size*; Cambridge University Press: New York, U.S.A., 1983.
- (43) Miller, D. R. *Biology of the Kaminuriak Population of barren-ground caribou Part 3*; Can. Wildl. Serv. Report Series No. 36; Ottawa, Canada, 1976.
- (44) Kuyt, E. *Food habits of wolves on the barren-ground caribou range*; Can. Wildl. Serv. Report; Ottawa, Canada, 1972.
- (45) Mech, D. *The Wolf: The Ecology And Behavior Of An Endangered Species*; Natural History Press: Garden City, NY, 1970.
- (46) McLachlan, M. S. *Environ. Sci. Technol.* **1994**, *28*, 2407.
- (47) Jodicke, B.; Ende, M.; Helge, H.; Neuber, D. *Chemosphere* **1992**, *25*, 1061.
- (48) McLachlan, M. S. *Toxicol. Appl. Pharm.* **1993**, *123*, 68.
- (49) Dauphine, T. C. *Biology of the Kaminuriak population of barren-ground caribou, Part 4: Growth, reproduction and nutritional condition*; Can. Wildl. Serv. Report; Ottawa, Canada, 1979.
- (50) Lavigueur, L.; Barrette, C. *Can. J. Zool.* **1992**, *70*, 1753.
- (51) Holleman, D. F.; Luick, J. R.; White, R. G. *J. Wildl. Manage.* **1979**, *43*, 192.
- (52) AMAP. *AMAP Assessment Report: Arctic Pollution Issues. Arctic Monitoring and Assessment Programme (AMAP)*; Oslo, Norway, 1998.
- (53) Bidleman, T. F.; Falconer, R. L.; Walla, M. D. *Sci. Total Environ.* **1995**, *160/161*, 55.
- (54) Strachan, W. unpublished data.
- (55) Wania, F. *Chemosphere* **1997**, *35*, 2345.
- (56) Muir, D. C. G.; Segstro, M. D.; Welbourne, P. M.; Toom, D.; Eisenreich, S. J.; Macdonald, C. R.; Whelpdale, D. M. *Environ. Sci. Technol.* **1993**, *27*, 1201.
- (57) Komp, P.; McLachlan, M. S. *Environ. Sci. Technol.* **1997**, *31*, 886.

Received for review November 20, 2002. Revised manuscript received March 28, 2003. Accepted March 31, 2003.

ES021035X